Aromatic Pathways in Carbathiaporphyrins

3 AUTHORS:

Rashid Valiev
Tomsk State University
22 PUBLICATIONS **86** CITATIONS

SEE PROFILE

Heike Fliegl
University of Oslo
36 PUBLICATIONS **852** CITATIONS

SEE PROFILE

Dage Sundholm
University of Helsinki
205 PUBLICATIONS **4,627** CITATIONS

SEE PROFILE

Aromatic Pathways in Carbathiaporphyrins

Rashid R. Valiev,*,[†,‡] Heike Fliegl,*,[§] and Dage Sundholm*,[∥]

[†]Tomsk Polytechnic University, 43a Lenin Avenue, Building 2, Tomsk 634050, Russian Federation

[‡]Tomsk State University, Lenina Avenue 36, Tomsk 634050, Russian Federation

[§]Centre for Theoretical and Computational Chemistry (CTCC), Department of Chemistry, University of Oslo, P.O. Box 1033, Blindern, Oslo 0315, Norway

[∥]Department of Chemistry, University of Helsinki, P.O. Box 55 (A.I. Virtanens plats 1), Helsinki FIN-00014, Finland

Ⓢ *Supporting Information*

ABSTRACT: Magnetically induced current densities and current pathways have been calculated for carbaporphyrins and carbathiaporphyrins using the gauge including magnetically induced current (GIMIC) method. The aromatic character and current pathways are obtained from the calculated current density susceptibilities. The current-density calculations show that five of the studied carbaporphyrinoids are aromatic, two are antiaromatic, and one is nonaromatic. The analysis of the current pathways of the investigated molecules reveals some general trends for the current flow in carbaporphyrinoids. Insertion of a CH_2 group into the all-carbon ring generally cuts or restricts the current flow, leading to a stronger current of the alternative pathway of the ring. No obvious trends regarding the current strengths and pathways of the thiophene and cyclopentadienyl rings were obtained. The present study shows that it is indeed difficult to predict the electron delocalization pathways of general carbaporphyrinoids. Thus, a careful analysis of the current density is necessary for determining their electron delocalization pathways.
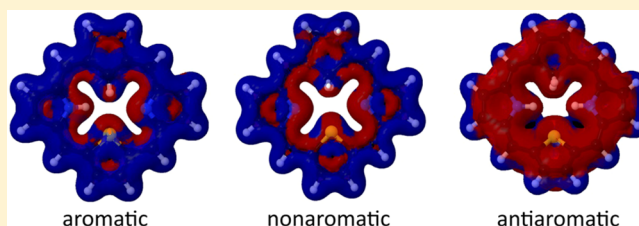
1. INTRODUCTION

N-Confused porphyrins are porphyrinoids with one inverted pyrrolic ring, making the heteroatom pointing outward from the macroring.[1,2] Porphyrins with one of the pyrrolic rings replaced by a five-membered unsaturated all-carbon ring are called *true carbaporphyrins*,[3] because N-confused porphyrins should be called carbaporphyrins according to the IUPAC nomenclature. Aronoff and Calvin as well as Pauling proposed carbaporphyrins already in the early 1940s,[4,5] whereas N-confused porphyrins were independently synthesized and characterized for the first time by the research groups of Furuta and Latos-Grażyński in 1994.[6,7] The first true carbaporphyrins were also synthesized in the mid 1990s.[1,8,9]

Carbaporphyrinoids are interesting molecules because of their aromatic properties as well as due to their ability to bind metal ions in unusual oxidation states, which makes them particularly attractive for catalysis.[1,3] Since the molecular structure of the carbaporphyrins is a combination of the classical porphyrin macroring motive and a heterocyclic compound, carbaporphyrins form a very unique chemical environment for metal complexation. The heteroatoms of the N-confused pyrrole moiety can vary, and different heterocyles involving, for example, oxygen, sulfur, or selenium have been synthesized.[1] Recently, Berlicka et al. managed to synthesize and characterize a number of true carbathiaporphyrins with one cyclopentadienyl ring and one thiophene ring replacing two of the pyrrolic rings.[3] Thus, the synthesized 21-carba-23-thiaporphyrin contains one cyclopentadienyl moiety in addition

to the thiophene ring and two pyrrolic rings. They characterized the molecules spectroscopically and assessed molecular aromaticity by measuring ^{1}H NMR chemical shifts. They also performed density functional theory (DFT) calculations of nucleus-independent chemical shifts (NICS).[3,10]

Although carbaporphyrinoids are interesting aromatic molecules with an unusual molecular structure and chemistry, very little is known about their aromatic character and electron delocalization pathways. Since it is hard to unambiguously quantify the electron delocalization of complicated multiring molecules experimentally, the determination of the current pathways relies on explicit calculations of the susceptibility of the magnetically induced current densities, which provide information about how electronic charge can be transported around the molecular rings.

In 2004, the gauge including magnetically induced current (GIMIC) method was developed.[11−13] GIMIC can be used for calculating magnetically induced current densities using gauge including atomic orbitals. The GIMIC method has since then been employed in a large number of studies showing that integration of the current-density susceptibility circling around molecular rings can be used as a reliable aromaticity index. The GIMIC method can also be used for assessing the electron-delocalization pathways by calculating the strength of the
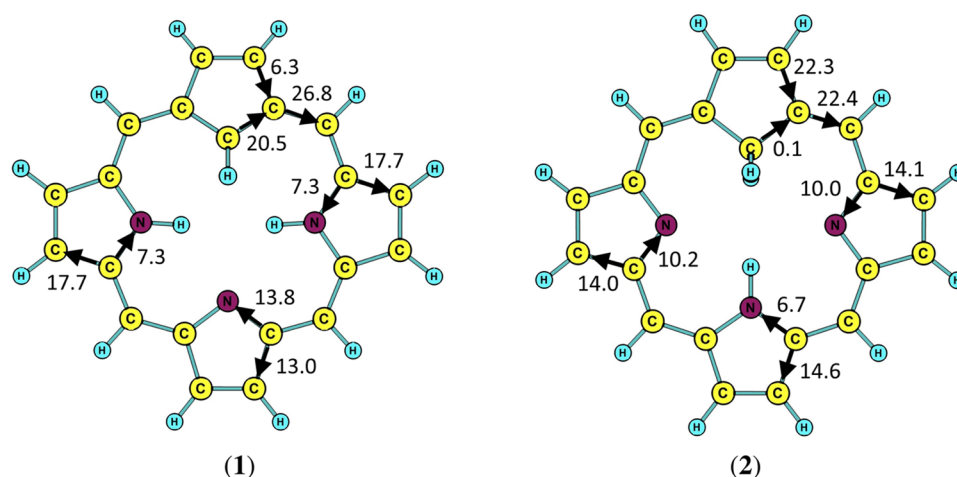
Figure 1. Molecular structures and calculated current strengths and current pathways (arrows) for the carbaporphyrins **1** and **2**.

currents passing selected chemical bonds when the molecule is exposed to an external magnetic field.[14−18] Therefore, analyses of calculated current densities have proven to be very useful for obtaining a more detailed picture of the aromatic pathways in porphyrinoids[19−23] as well as for other complicated multiring systems.[15−17,24−27] For an overview of the GIMIC method and its applications, the reader is referred to ref 13.

The aim of the present study is to perform explicit calculations of the magnetically induced current density for determining the pathways of the magnetically induced currents, which are also considered to be electron-delocalization pathways of the molecules. Detailed knowledge of the current pathways may lead to a better understanding of the aromatic properties, in particular when aiming at the design of porphyrinoids with distinct properties.

The paper is organized as follows. The computational methods and molecular structures of the studied molecules are presented in sections 2 and 3, respectively. The calculated nuclear magnetic resonance (NMR) shieldings of the protons are compared to experimental data in section 4. The calculated magnetically induced current densities are discussed in section 5. The final conclusions of the study are drawn in section 6.

2. COMPUTATIONAL METHODS

The molecular structures were optimized at the density functional theory (DFT) level using the B3LYP functional[28,29] as implemented in Turbomole 6.5.[30] The Karlsruhe triple-ζ quality basis sets (def2-TZVP) were employed.[31,32] The mpshift module of Turbomole was used in the calculations of the nuclear magnetic shieldings at the B3LYP level using the def2-TZVP and split-valence polarization basis (def2-SVP) sets.[31,33,34] Tetramethylsilane (TMS) was used as reference substance in the calculations of NMR chemical shifts. The B3LYP/def2-TZVP nuclear magnetic shielding for the TMS hydrogens is 31.91 ppm.[35]

Magnetically induced current densities were calculated at the B3LYP/def2-SVP and B3LYP/def2-TZVP levels using the GIMIC program.[11−13] GIMIC is an independent program that uses the atomic orbital density matrix as well as the corresponding first-order magnetically perturbed density matrices from the nuclear magnetic shielding calculations and basis-set information as input data.[11,12] Since GIMIC uses gauge-including atomic orbitals (GIAO), calculations using standard basis sets yield accurate gauge-origin independent current densities.[36,37]

Integration of the current flow passing planes that cut the chemical bonds of interest yields the current-strength susceptibilities (in nAT^{-1}) along the considered chemical bonds. The current-strength susceptibility is for simplicity in the following called current strength. The molecular pictures of the current pathways were obtained with ChemCraft version 1.7.[38]

3. MOLECULAR STRUCTURES AND NOMENCLATURE

The molecular structure of **1** can be derived from the porphin structure by replacing a pyrrolic ring without an inner hydrogen with an isoelectronic cyclopentadienyl ring. The cyclopentadienyl ring is tilted 15° out from the plane with the inner CH hydrogen bent an additional 13° out from the cyclopentadienyl plane.

The molecular structure of **2** can be derived from porphin by replacing an inner NH moiety with an isoelectronic CH$_2$ group yielding a cyclopentadiene ring, which cuts the inner route of the conjugation pathway. **2** is practically planar with only the two inner hydrogens pointing out from the porphyrinoid plane. The molecular structures of the true carbaporphyrins **1** and **2** are shown in Figure 1.

The molecular structure of **3** can be derived from porphin by replacing one of the pyrrolic rings with an inner hydrogen with a formally isoelectronic thiophene moiety and a pyrrolic ring without an inner hydrogen is replaced by an isoelectronic cyclopentadienyl ring. **3** has one hydrogen attached to the inner carbon and the second inner hydrogen attached to the nitrogen of one of the pyrrolic rings. The conjugation pathway of **3** can pass either the inner carbon or the β carbons. However, the C=C double bond between the β carbons is formally decoupled from the conjugation pathway of the macroring. Thus, the formal conjugation pathway of **3** passes the inner carbon of the cyclopentadienyl ring. The macroring is slightly bowed with the inner hydrogens pointing a few degrees out from the plane. Carbathiaporphyrin **3** has very recently been synthesized by Berlicka et al.[3]

The molecular structure of **4** can be derived from porphin by replacing the pyrrolic rings with an inner hydrogen with a cyclopentadiene ring and a thiophene moiety, respectively. The saturation of the inner carbon of the cyclopentadiene ring cuts the inner conjugation pathway. The macroring is practically
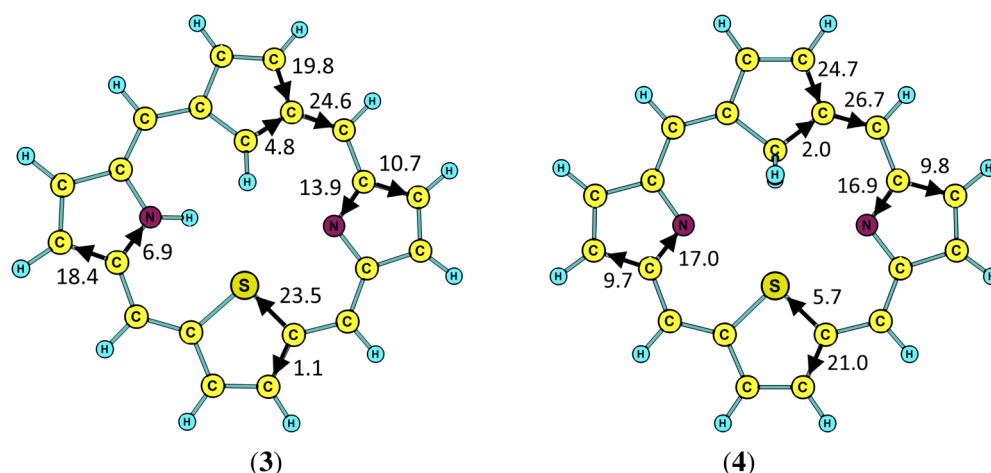
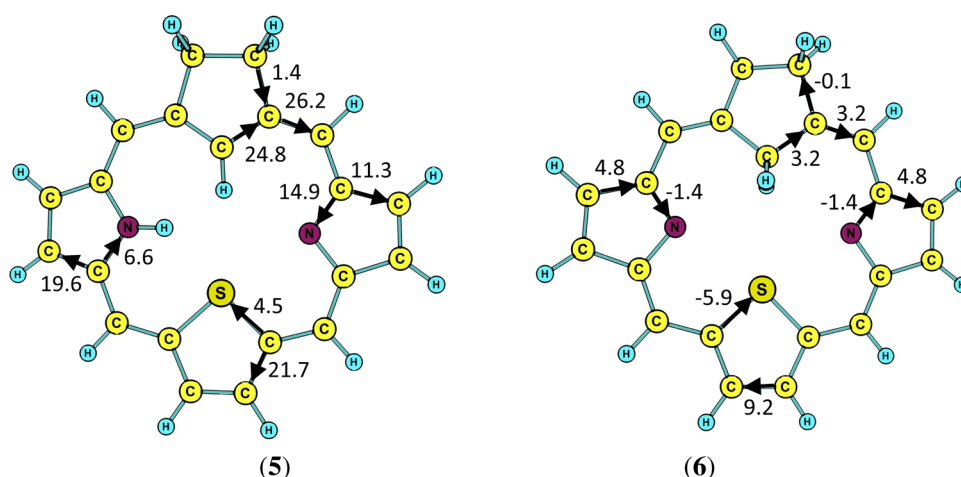**Figure 2.** Molecular structures and calculated current strengths and current pathways (arrows) for the carbathiaporphyrins **3** and **4**.

Figure 3. Molecular structures and calculated current strengths and current pathways (arrows) for the carbathiaporphyrins **5** and **6**.
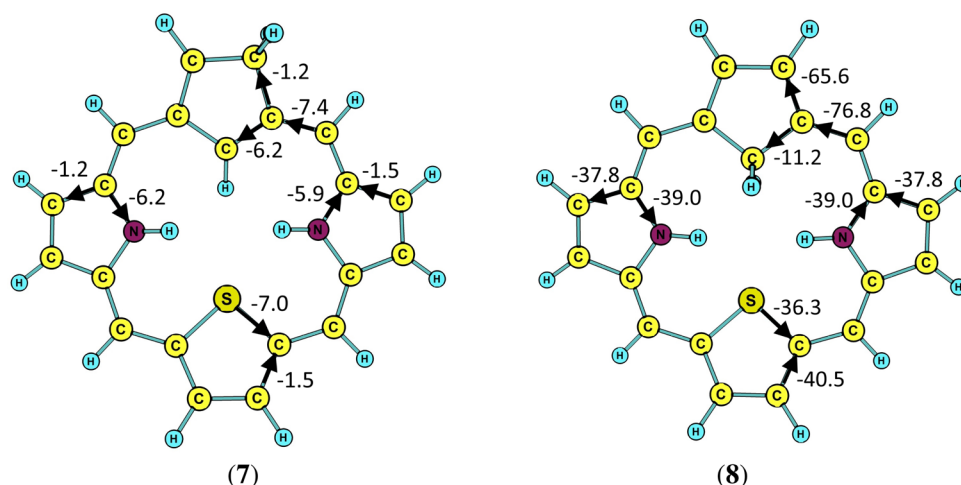

Figure 4. Molecular structures and calculated current strengths and current pathways (arrows) for the carbathiaporphyrins **7** and **8**.

planar with the two inner hydrogens pointing out from the plane. The molecular structures of carbathiaporphyrins **3** and **4** are shown in Figure 2.

The molecular structure of **5** can be derived from chlorin by replacing an NH moiety with S, and a CH group replaces the nitrogen of the five-membered ring that has a saturated C_β–C_β

bond. The macroring of **5** is almost planar with only the hydrogens of C_β pointing out from the plane. Carbathiaporphyrin **5** has very recently been synthesized by Berlicka et al.[3]

The molecular structure of **6** can be derived from chlorin by replacing the two inner NH groups with S and CH$_2$ moieties. The macroring is largely planar with only the sp^3-hybridized C_β
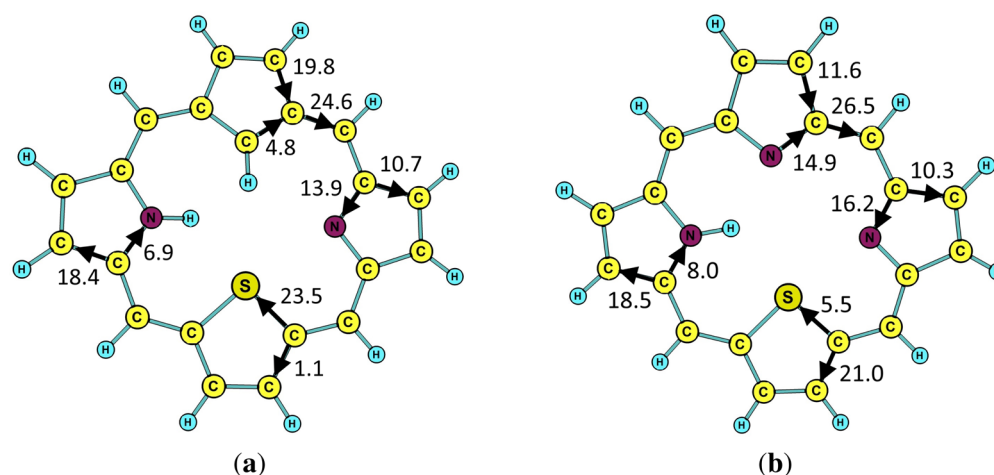
C

Figure 5. Comparison of the calculated current strengths and current pathways (arrows) for (a) carbaporphyrin **3** and (b) the corresponding porphyrinoid **9**.

Table 1. Calculated and Experimental ^{1}H NMR Chemical Shifts for the Carbaporphyrins 3 and 5^a

	carbathiaporphyrin 3		carbathiaporphyrin 5	
position	calculated	experimental[3]	calculated	experimental[3]
1−2	8.61; 8.54; (8.58)	8.26	5.44; 5.50; 5.32; 5.26; (5.38)	4.91
3−4	10.39; 10.40; (10.40)	9.92	10.15; 10.29; (10.22)	9.45
5−6	9.58; 9.48; (9.53)	9.01	9.45; 9.45; (9.45)	8.84
7−8	9.49; 9.34; (9.42)	8.44	9.70; 9.51; (9.61)	8.51
9−10	10.20; 10.36; (10.28)	9.17	10.40; 10.48; (10.44)	9.16
11	−6.90	−4.84	−8.00	−5.16
12	−5.67	−5.32	−6.80	−3.7

^{a}The average chemical shifts for the almost equivalent protons are given within parentheses.

carbons bent out from the plane. The hydrogens of the CH$_2$ moiety are also pointing out from the porphyrinoid plane. The structures of carbathiaporphyrins **5** and **6** are shown in Figure 3.

The molecular structure of **7** can be derived from porphin by replacing one of the pyrrole nitrogens without an inner hydrogen with S and the other with a CH moiety. The conjugation pathway passes the inner carbon of the five-membered carbon ring, because one of the C$_\beta$ carbons is saturated. The structure of **7** corresponds to a porphyrinoid with three inner hydrogens, suggesting that its aromatic character qualitatively differs from that of porphin. The porphyrinoid ring is bent with the sulfur atom of the thiophene ring and the inner hydrogens slightly out of the plane. The two hydrogens of the saturated carbon also point out from the plane of the all-carbon five-membered ring.

The molecular structure of **8** has four inner hydrogens, two of them are attached to the inner carbon of the five-membered carbon ring, and the other two are attached to the pyrrolic rings. **8** has two extra inner hydrogens as compared to **3** and **4**, suggesting that its aromatic character is qualitatively different from that of **3** and **4**. The porphyrinoid ring is largely planar with the thiophene ring tilted 25° out from the plane of the macromolecule. The hydrogens of the pyrrolic rings lie in the porphyrin plane, and the CH$_2$ hydrogens point out from the plane of the macrocycle. The molecular structures of the carbathiaporphyrins **7** and **8** are shown in Figure 4.

The molecular structure of **9** has been obtained by replacing the inner CH moiety of **3** with a nitrogen atom. Thiaporphyrin **9** is included in the study for comparison with the corresponding carbathiaporphyrin **3**. The structure of **9** is shown in Figure 5. The Cartesian coordinates of the studied molecules are given as Supporting Information.

4. ^{1}H NMR CHEMICAL SHIFTS

The calculated ^{1}H NMR chemical shifts of the outer and inner hydrogens of the carbathiaporphyrins **3** and **5** are compared to available experimental data[3] in Table 1. The labeling of the hydrogen atoms is shown in Figure 6. The calculated chemical
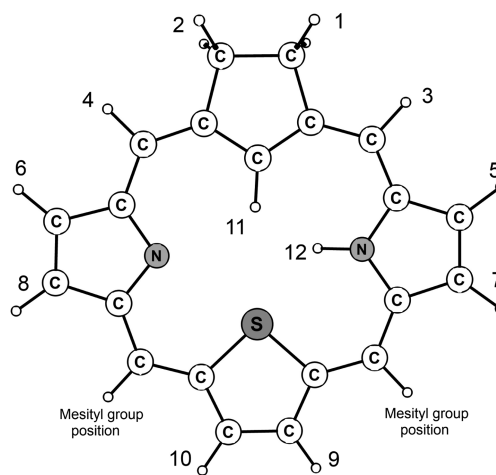

Figure 6. Position and labeling of the protons of the carbaporphyrins **3** and **5**. The two mesityl groups of the synthesized molecules have been omitted for clarity.

D

shifts agree rather well with the measured ones. However, the calculated ^{1}H NMR chemical shifts for the outer hydrogens are generally somewhat larger than the measured ones, and the calculated ^{1}H NMR chemical shifts for the inner hydrogens are smaller than those obtained in the experiment. Thus, the ring currents are most likely slightly weaker under experimental conditions than obtained in the calculations. However, there must also be other reasons for the differences between calculated and measured chemical shifts, because solely the ring current effect would lead to an almost constant shift in the nuclear magnetic shieldings of the hydrogens at the β carbons. The large discrepancy for the inner hydrogens may be due to time-average effects, because the inner protons are not stationary in porphyrinoids at room temperature.[39] Interactions with the solvent molecules may also have a large impact on the ^{1}H NMR chemical shifts of the inner hydrogens. It is hard to consider solvent effects in calculations of magnetic properties because time-averaged electrostatic and current effects have to be taken into account.[40] However, current densities calculations for the porphyrinoids in the gas phase yield qualitatively the correct aromatic pathways and degree of aromaticity as demonstrated in our previous studies.[19−23] The calculated isotropic NMR shielding constants are given as Supporting Information.

5. CURRENT-DENSITY CALCULATIONS

Analysis of the calculated current densities provides current pathways and the aromatic character of the studied molecules. The strength of the currents passing selected chemical bonds was obtained by numerical integration as explained in the Computational Methods section. Kirchhoff's law is fulfilled for most of the studied molecules. The largest discrepancies of 1.8 nAT^{-1} were obtained for **1** and **2**, which is most likely due to the numerical integration as it may be hard to place the rectangular integration grid in a multiring molecule such that only the desired current contributions are taken into account. For **3**, the current strength passing one of the pyrrolic rings is 0.7 nAT^{-1} larger than for other bonds of the porphyrinoid ring, whereas for all other bonds Kirchhoff's law is fulfilled within 0.1 nAT^{-1}.

The influence of the mesityl groups on the ring-current strengths was assessed by performing calculations at the B3LYP/def2-SVP level. The calculations showed that the mesityl groups have a negligible effect on the current strengths. The mesityl groups were therefore omitted in the subsequent current-density calculations at the B3LYP level, which were performed using the larger def2-TZVP basis sets. The chosen structures represent the experimentally studied carbathiaporphyrins and other molecules of this class of compounds.

Current densities in a plane 1 bohr above the molecular plane are visualized in the Supporting Information. The current density plots do not provide any insights that cannot be deduced from the current strength analysis.

5.1. Carbaporphyrins 1 and 2. **1** and **2** are the basic carbaporphyrins with a cyclopentadienyl and a cyclopentadiene ring fused into the porphyrinoid ring, respectively. The current strengths calculated for **1** and **2** are shown in Figure 1. For **1**, the ring-current strength around the macroring is 26.8 nAT^{-1}, which is as large as for porphin.[19] The ring current splits at the pyrrolic rings into an inner and outer pathway as for porphin. The pyrrole nitrogen with an inner hydrogen has a larger resistance than the one without the hydrogen. For the pyrrolic ring without inner hydrogen, the current strength is about the

same size along the two routes, whereas for the pyrrolic ring with an inner hydrogen the current strength on the outside of the ring is 17.7 nAT^{-1} as compared to the current strength of 7.3 nA^{-1} on the inside of the ring. At the cyclopentadienyl ring, the current prefers the inner route, whose current strength is 20.5 nAT^{-1}. The current strength along the outer pathway is 6.3 nAT^{-1}. Thus, the conductivity of the CH unit is even better than for the isoelectronic nitrogen.

The total ring current strength of **2** is 22.4 nAT^{-1}, which is slightly weaker than for **1** and porphin.[19] The inner CH$_2$ unit of the cyclopentadiene ring of **2** completely cuts the current pathway. For the pyrrolic rings without an inner hydrogen, the current strengths along the inner and outer routes are almost the same differing by only 4 nAT^{-1}, whereas for the pyrrolic ring with an inner hydrogen the current prefers the outer pathway as for **1**.

5.2. Carbathiaporphyrins 3 and 4. The carbathiaporphyrin structures **3** and **4** are obtained from **1** and **2** by replacing a pyrrolic ring with an inner hydrogen with a thiophene ring. The calculated current strengths and current pathways for **3** and **4** are given in Figure 2. The ring-current strength of **3** is 24.6 nAT^{-1}, which is only 2.4 nAT^{-1} weaker than for porphin. **4** sustains a current strength of 26.7 nAT^{-1}, which is practically the same as for porphin.[19]

Even though **1** and **3** are formally isoelectronic and structurally similar, the current pathways significantly differ. The current passing the inner CH unit of **3** is only 4.8 nAT^{-1} as compared to 20.5 nAT^{-1} in **1**. At the thiophene ring of **3**, the main current flow passes the sulfur atom and only a very weak current of 1.1 nAT^{-1} takes the outer route. The two pyrrolic rings have qualitatively the same current pattern as usually obtained for porphyrins. The current pathways of **4** remind us of those for the formally isoelectronic **2**. The current pathways at the thiophene are completely different for **3** and **4**. In **3** almost no current passes along the outer pathway, whereas in **4** the current strength of 21.0 nAT^{-1} along the outer pathway is more than three times stronger than the current passing the sulfur atom.

Replacing the inner CH moiety of carbathiaporphyrin **3** with the isoelectronic N yields thiaporphyrin **9**. The substitution increases the current strength of the macroring from 24.6 to 26.5 nAT^{-1}, which is almost the same current strength as for porphin. For **3**, the main current of 23.5 nAT^{-1} passes the sulfur atom, whereas for **9** the current passing on the outside of the thiophene ring is 21.0 nAT^{-1} and only 5.5 nAT^{-1} takes the inner route. The ring current in **9** is almost equally split at the pyrrole rings without an inner hydrogen. The current strengths along the inner pathways of 14.9 and 16.2 nAT^{-1}, respectively, are somewhat larger than those along the outer route of 11.6 and 10.3 nAT^{-1}. The current strengths and pathways of **3** and **9** are compared in Figure 5.

5.3. Carbathiaporphyrins 5 and 6. In **5** and **6**, the outer conjugation pathway of the all-carbon ring is blocked by saturating the β carbons of **3** and **4**, respectively. The calculated current strengths and current pathways for **5** and **6** are given in Figure 3.

The saturation of the β carbons of the all-carbon ring prevents the ring current of both molecules to take that route. The total net current strength of **5** is 26.2 nAT^{-1}, implying that it is almost as aromatic as porphin. The current pattern of **5** at the pyrrolic rings is the same as that generally obtained for porphyrins. The current prefers the outer route at the pyrrolic ring with an inner hydrogen. The current strength via the β

carbons is 19.6 nAT^{-1} as compared to 6.6 nAT^{-1} along the inner pathway, whereas for the pyrrolic ring without an inner hydrogen the ring current is almost equally divided between the two routes. At the thiophene ring of **5**, the main current flow passes the β carbons, whereas only 4.5 nAT^{-1} takes the inner route via the sulfur atom. Thus, the current flows of **4** and **5** are very similar, even though the structures of the all-carbon rings are completely different.

6 is weakly aromatic or nonaromatic, because it sustains a very small ring current of 3.2 nAT^{-1}. Actually, it is remarkable that **6** sustains even a weak ring current, because both the inner and the outer pathways are cut by saturated carbons at the all-carbon ring. The pyrrolic rings sustain weak ring currents of their own, since paratropic (negative) currents of -1.4 nAT^{-1} pass the nitrogen. The ring current around the thiophene ring of -5.9 nAT^{-1} is one-half the ring-current strength of benzene.

5.4. Carbathiaporphyrins 7 and 8. Carbathiaporphyrins **7** and **8** have three and four inner hydrogens, respectively. The outer conjugation of **7** is cut by saturating one of the β carbons. Their aromatic properties are therefore expected to differ from the rest of the studied molecules. The calculated current strengths and current pathways for **7** and **8** are given in Figure 4.

7 is weakly antiaromatic according to the ring-current criterion, sustaining a ring current of -7.4 nAT^{-1}. A weak current of -1.2 nAT^{-1} passes the saturated β carbon of the all-carbon ring, whereas the current strength along the inner pathway is -6.2 nAT^{-1}. The two pyrrolic rings have similar current strengths of -5.9 nAT^{-1} along the inner route, whereas -1.5 nAT^{-1} takes the outer pathway. At the thiophene ring, the stronger current also takes the inner route. Thus, the main current pathway of the net paratropic current is along the inner cross of the carbathiaporphyrin.

8 is strongly antiaromatic, sustaining a net paratropic current of -76.8 nAT^{-1}, which is the strongest paratropic current strength calculated for a porphyrinoid so far.[21−23] The current is almost equally divided at the pyrrolic rings and at the thiophene ring. The current flow is significantly affected by the CH_2 group of the cyclopentadiene ring, which has a current strength of -65.6 nAT^{-1} along the outer pathway. However, a rather strong current of -11.2 nAT^{-1} passes the sp^3-hybridized inner carbon.

6. SUMMARY AND CONCLUSIONS

Magnetically induced current densities and current pathways have been calculated and analyzed for a set of true carbaporphyrinoids and carbathiaporphyrins. The aromatic character of the investigated set of molecules has been determined by assuming that the magnetic ring-current criterion holds. The investigated molecules **1−5** are found to be aromatic, while **6** is nonaromatic, and **7** and **8** are antiaromatic. The analysis of the current pathways of the investigated molecules revealed some general trends. The ring current splits at the subrings of the porphyrinoids, implying that all π-electrons are participating in the current pathway. Similar results have previously been obtained for other porphyrinoids.[19−23] For pyrrolic rings with an inner hydrogen, a stronger current passes along the outer route via the C_β=C_β bond, when the porphyrinoid is aromatic, whereas for antiaromatic porphyrinoids, the paratropic current prefers the inner pathway. For pyrrolic rings without an inner hydrogen, the current is nearly equally divided between the inner and the

outer pathways. However, the current strength along the inner route is usually slightly larger.

Any obvious trends regarding the current strengths and pathways of the thiophene ring are not found among the investigated molecules. The insertion of a CH_2 group into the all-carbon ring generally cuts or restricts the current flow, leading to a stronger current on the other side of the ring.

For carbathiaporphyrin **3**, which has an inner CH moiety, the current flows mainly on the outside of the all-carbon ring along the C_β=C_β bond, which is somewhat unexpected, because CH is isoelectronic with N, which is an integrated part of the current pathway of porphin. Replacing the CH moiety with nitrogen leads to a similar current flow as observed for porphin.

However, for carbaporphyrin **1**, the main current flow passes indeed the inner CH moiety of the all-carbon ring. The current strengths passing selected chemical bonds of the studied molecules are summarized in Table S1, Supporting Information.

As seen in previous studies of the current pathways of porphyrinoids as well as in the present study of the current pathways of the carbaporphyrins and carbathiaporphyrins, it is very hard to predict the electron delocalization pathways of such multiring molecules. A careful theoretical analysis of the current pathway is therefore necessary to get deeper insights and a more clear picture of the electron delocalization pathways in this kind of molecules. Further investigations on similar porphyrinoid model compounds are planned with the aim to obtain general trends that can be used for predicting the aromatic character of novel carbaporphyrinoids.

■ ASSOCIATED CONTENT

⑤ Supporting Information

Cartesian coordinates and calculated isotropic nuclear magnetic shielding constants of the studied molecules. This material is available free of charge via the Internet at http://pubs.acs.org.

■ AUTHOR INFORMATION

Corresponding Authors

*E-mail: valievrashid@mail.ru.

*E-mail: Heike.Fliegl@kjemi.uio.no.

*E-mail: Dage.Sundholm@helsinki.fi.

Notes

The authors declare no competing financial interest.

■ ACKNOWLEDGMENTS

■ REFERENCES

(1) Pawlicki, M.; Latos-Grażyński, L. O-confusion approach in construction of carbaporphyrinoids. *Chem. Rec.* **2006**, *6*, 64−78.

(2) Ghosh, A. A Perspective of One-Pot Pyrrole-Aldehyde Condensations as Versatile Self-Assembly Processes. *Angew. Chem., Int. Ed.* **2004**, *43*, 1918−1931.

(3) Berlicka, A.; Dutka, P.; Szterenberg, L.; Latos-Grażyński, L. Towards True Carbaporphyrinoids: Synthesis of 21-Carba-23-thiaporphyrin. *Angew. Chem., Int. Ed.* **2014**, *53*, 4885−4889.

(4) Aronoff, S.; Calvin, M. The Porphyrin-Like Products Of The Reaction Of Pyrrole With Benzaldehyde. *J. Org. Chem.* **1943**, *8*, 205−223.

(5) Senge, M. O. Extroverted Confusion-Linus Pauling, Melvin Calvin, and Porphyrin Isomers. *Angew. Chem., Int. Ed.* **2011**, *50*, 4272−4277.

(6) Furuta, F.; Asano, T.; Ogawa, T. N-Confused Porphyrin: A New Isomer of Tetraphenylporphyrin. *J. Am. Chem. Soc.* **1994**, *116*, 767−768.

(7) Chmielewski, P. J.; Latos-Grażyński, L.; Rachlewicz, K.; Glowiak, T. Tetra-p-tolylporphyrin with an Inverted Pyrrole Ring: A Novel Isomer of Porphyrin. *Angew. Chem., Int. Ed.* **1994**, *33*, 779−781.

(8) Berlin, K. Carbaporphyrins. *Angew. Chem., Int. Ed.* **1996**, *35*, 1820−1822.

(9) Lash, T. D.; T.Chaney, S. Oxypyriporphyrin, the First Fully Aromatic Porphyrinoid Macrocycle with a Pyridine Subunit. *Chem.— Eur. J.* **1996**, *2*, 944−948.

(10) von Ragué Schleyer, P.; Maerker, C.; Dransfeld, A.; Jiao, H.; van Eikema Hommes, N. J. R. Nucleus-Independent Chemical Shifts: A Simple and Efficient Aromaticity Probe. *J. Am. Chem. Soc.* **1996**, *118*, 6317−6318.

(11) Jusélius, J.; Sundholm, D.; Gauss, J. Calculation of Current Densities using Gauge-Including Atomic Orbitals. *J. Chem. Phys.* **2004**, *121*, 3952−3963.

(12) Taubert, S.; Sundholm, D.; Jusélius, J. Calculation of spin-current densities using gauge-including atomic orbitals. *J. Chem. Phys.* **2011**, *134*, 054123.

(13) Fliegl, H.; Taubert, S.; Lehtonen, O.; Sundholm, D. The gauge including magnetically induced current method. *Phys. Chem. Chem. Phys.* **2011**, *13*, 20500−20518.

(14) Fliegl, H.; Sundholm, D.; Taubert, S.; Jusélius, J.; Klopper, W. Magnetically Induced Current Densities in Aromatic, Antiaromatic, Homoaromatic, and Nonaromatic Hydrocarbons. *J. Phys. Chem. A* **2009**, *113*, 8668−8676.

(15) Taubert, S.; Sundholm, D.; Jusélius, J.; Klopper, W.; Fliegl, H. *J. Phys. Chem. A* **2008**, *112*, 13584−13592.

(16) Fliegl, H.; Sundholm, D.; Taubert, S.; Pichierri, F. Aromatic Pathways in Twisted Hexaphyrins. *J. Phys. Chem. A* **2010**, *114*, 7153−7161.

(17) Fliegl, H.; Sundholm, D.; Pichierri, F. Aromatic Pathways in Mono- and Bisphosphorous Singly Möbius Twisted [28] and [30]Hexaphyrins. *Phys. Chem. Chem. Phys.* **2011**, *13*, 20659−20665.

(18) Fliegl, H.; Lehtonen, O.; Sundholm, D.; Kaila, V. R. I. Hydrogen-bond strengths by magnetically induced currents. *Phys. Chem. Chem. Phys.* **2011**, *13*, 434−437.

(19) Fliegl, H.; Sundholm, D. Aromatic Pathways of Porphins, Chlorins and Bacteriochlorins. *J. Org. Chem.* **2012**, *77*, 3408−3414.

(20) Fliegl, H.; Özcan, N.; Mera-Adasme, R.; Pichierri, F.; Jusélius, J.; Sundholm, D. Aromatic pathways in thieno-bridged porphyrins: understanding the influence of the direction of the thiophene ring on the aromatic character. *Mol. Phys.* **2013**, *111*, 1364−1372.

(21) Valiev, R. R.; Fliegl, H.; Sundholm, D. Insights into Magnetically Induced Current Pathways and Optical Properties of Isophlorins. *J. Phys. Chem. A* **2013**, *117*, 9062−9068.

(22) Valiev, R. R.; Fliegl, H.; Sundholm, D. The aromatic character of thienopyrrole-modified 20π-electronporphyrinoids. *Phys. Chem. Chem. Phys.* **2014**, *16*, 11010−11016.

(23) Fliegl, H.; Pichierri, F.; Sundholm, D. Antiaromatic Character of 16 π Electron Octaethylporphyrins: Magnetically Induced Ring Currents from DFT-GIMIC Calculations. *J. Phys. Chem. A* **2015**, doi: 10.1021/jp5067549.

(24) Taubert, S.; Sundholm, D.; Pichierri, F. Magnetically Induced Currents in [n]Cycloparaphenylenes, n = 6−11. *J. Org. Chem.* **2010**, *75*, 5867−5874.

(25) Sundholm, D. C_{72}: Gaudiene a Hollow and Aromatic All-Carbon Molecule. *Phys. Chem. Chem. Phys.* **2013**, *15*, 9025−9028.

(26) Valiev, R. R.; Cherepanov, V. N. The Influence of Benzene Rings on Aromatic Pathways in the Porphyrins. *Int. J. Quantum Chem.* **2013**, *113*, 2563−2567.

(27) Baryshnikov, G. V.; Valiev, R. R.; Karaush, N. N.; Minaev, B. F. Aromaticity of the planar hetero[8]circulenes and their doubly charged ions: NICS and GIMIC characterization. *Phys. Chem. Chem. Phys.* **2014**, *16*, 15367−15374.

(28) Becke, A. D. Density-functional thermochemistry. III. The role of exact exchange. *J. Chem. Phys.* **1993**, *98*, 5648−5652.

(29) Lee, C.; Yang, W.; Parr, R. G. Development of the Colle-Salvetti correlation-energy formula into a functional of the electron density. *Phys. Rev. B* **1988**, *37*, 785−789.

(30) Furche, F.; Ahlrichs, R.; Hättig, C.; Klopper, W.; Sierka, M.; Weigend, F. Turbomole. *WIREs Comput. Mol. Sci.* **2014**, *4*, 91−100.

(31) Schäfer, A.; Horn, H.; Ahlrichs, R. Fully Optimized Contracted Gaussian-Basis Sets for Atoms Li to Kr. *J. Chem. Phys.* **1992**, *97*, 2571−2577.

(32) Weigend, F.; Ahlrichs, R. Balanced basis sets of split valence, triple zeta valence and quadruple zeta valence quality for H to Rn: Design and assessment of accuracy. *Phys. Chem. Chem. Phys.* **2005**, *7*, 3297−3305.

(33) Häser, M.; Ahlrichs, R.; Baron, H. P.; Weis, P.; Horn, H. Direct computation of 2nd-order SCF properties of large molecules on workstation computers with an application to large carbon clusters. *Theoret. Chim. Acta* **1992**, *83*, 455−470.

(34) Kollwitz, M.; Häser, M.; Gauss, J. Non-Abelian point group symmetry in direct second-order many-body perturbation theory calculations of NMR chemical shifts. *J. Chem. Phys.* **1998**, *108*, 8295−8301.

(35) Taubert, S.; Konschin, H.; Sundholm, D. Computational studies of ^{13}C NMR chemical shifts of saccharides. *Phys. Chem. Chem. Phys.* **2005**, *7*, 2561−2569.

(36) Ditchfield, R. Self-Consistent Perturbation-Theory Of Diamagnetism 0.1. Gauge-Invariant LCAO Method For NMR Chemical-Shifts. *Mol. Phys.* **1974**, *27*, 789−807.

(37) Wolinski, K.; Hinton, J. F.; Pulay, P. Efficient implementation of the gauge-independent atomic orbital method for NMR chemical shift calculations. *J. Am. Chem. Soc.* **1990**, *112*, 8251−8260.

(38) Zhurko, G. A.; Zhurko, D. A. http://www.chemcraftprog.com/.

(39) Braun, J.; Schlabach, M.; Wehrle, B.; Köcher, M.; Vogel, E.; Limbach, H.-H. NMR Study of the Tautomerism of Porphyrin Including the Kinetic HH/HD/DD Isotope Effects in the Liquid and the Solid State. *J. Am. Chem. Soc.* **1994**, *116*, 6593−6604.

(40) Özcan, N.; Mares, J.; Sundholm, D.; Vaara, J. Solvation chemical shifts of perylenic antenna molecules from molecular dynamics simulations. *Phys. Chem. Chem. Phys.* **2014**, *16*, 22309−22320.